

Ultrafast light-induced dichroism in silver nanoparticles

M. H. G. Miranda, E. L. Falcão-Filho, J. J. Rodrigues, Jr, Cid B. de Araújo, and L. H. Acioli*
Departamento de Física, Universidade Federal de Pernambuco, 50670-901 Recife, PE, Brazil
 (Received 27 May 2004; revised manuscript received 17 August 2004; published 7 October 2004)

Ultrafast light-induced dichroism in silver nanoparticles is studied. Two differently prepared colloids are examined: one sample has a broad distribution of sizes and shapes of silver nanoparticles, while the second sample, which is processed by laser ablation, presents a more uniform size and shape distribution (greater fraction of spherical particles). The experiments are performed with a femtosecond laser in a two-color, polarization-resolved, pump-probe setup. For the pristine colloid the signal amplitudes for the parallel and perpendicular polarizations present different behaviors as a function of the probe photon energy, which is not observed for the laser ablated samples. The temporal response of the samples is also different, with the laser ablated samples presenting faster electronic cooling rates. A model describing the induced dichroism that takes into account the shape of the colloid particles is presented. The effects of the size distribution are also discussed.

DOI: 10.1103/PhysRevB.70.161401

PACS number(s): 78.47.+p, 73.20.Mf, 81.40.Tv

Large interest has been directed to the optical response of metallic nanoparticles (NP) hosted in a dielectric medium. The reason for this is the enhancement of nonlinear optical properties of these materials due to local-field effects, initially studied in metallic surfaces.^{1,2} On the other hand, ultrafast optical studies of metals using femtosecond techniques have proven to be very effective in the understanding of the electron-electron and electron-phonon interactions in bulk,³⁻⁵ allowing to describe in detail the temporal evolution of a nonequilibrium photoexcited electronic distribution in the noble metals. Due to their technological importance, focus has also been given to the time response of nanostructured metallic systems, such as NP dispersed in a transparent host medium.⁶⁻¹² As an example, it has been demonstrated that the electronic properties can be modified, even though strictly quantum confinement effects may not be present. Some of the reported observations are the dependence of the electron-electron and electron-phonon interactions with particle size.^{13,14} For this class of materials attention must be given to the fact that elementary excitations that are not present, or are not optically accessible, in bulk may introduce additional difficulties. This is the case of surface-plasmon excitations in noble-metal NP, which have been studied by many groups.

In this communication we concentrate on an aspect that has not been previously addressed, which is the interaction of ultrashort pulses with a distribution of nonspherical silver NP in a colloid. Silver particles are interesting, because the threshold for the interband transition ($\Omega_{IB} \approx 4$ eV) is far from the surface-plasmon resonance (SPR) ($\Omega_{SPR} \approx 3$ eV), which facilitates the interpretation of the experimental data. We use two different colloids: one that is prepared by laser ablation, and a pristine colloid (as prepared). The colloids are initially prepared according to the procedure described in Ref. 15: 90 mg of AgNO_3 are diluted in 500 ml of water at 100 °C. A solution at 1% of sodium citrate 10 ml is added for reducing Ag, and later boiled and strongly stirred for 1 h. Subsequently, laser ablation is performed by placing a cuvette with the pristine colloid in front of the second harmonic of a

Q-switched Nd:YAG laser ($\lambda = 532$ nm, 10-Hz repetition rate and 8-ns pulse duration) for 1 h, where it was also stirred. The laser ablated colloid presents a more uniform distribution in both size and shape, with a large fraction ($>70\%$) of spherical NP. In the pristine colloid, the shapes and sizes of the NP are significantly nonuniform, and this is reflected in the results of the transient transmission measurements reported here.

A femtosecond Ti:sapphire laser generating pulses of ≈ 100 fs, repetition rate of 82 MHz, and operating around $\lambda \approx 800$ nm, was used in the time and polarization-resolved transient transmission measurements. The fundamental wavelength was used as the pump pulse with photon energy $\hbar\omega \approx 1.5$ eV, while the second harmonic was used as a probe pulse with photon energy $2\hbar\omega \approx 3$ eV (ratio of probe to pump power greater than 50). This scheme has the advantage of pumping below both the threshold for one-photon interband transition and the SPR; $\hbar\omega < \hbar\Omega_{IB}$, $\hbar\omega < \hbar\Omega_{SPR}$. A combination of a photoelastic modulator and polarizer are used to modulate the pump beam at a frequency of 100 kHz, and with this detection scheme we are able to detect fractional transmission changes, $\Delta T/T$, of the order of 10^{-5} . The probe pulse polarization is set to an angle of 45° , respective to that of the pump beam, and after the sample a polarizing beam splitter sends the parallel and perpendicular components to two detectors. The two signals are processed by a lock-in amplifier and separately recorded. In the time-resolved measurements the average pump powers at the sample were kept at ≈ 200 mW, corresponding to a fluence of ≈ 0.27 mJ/cm². Tests with thin films of silver and gold reveal no difference between the two orthogonal components, within our experimental resolution. The traces for both colloidal samples were recorded for probe photon energies varying between 2.95 and 3.22 eV.

Figure 1 shows the linear absorption spectra for (a) the laser ablated colloid and (b) the pristine colloid. The fact that the plasmon band (SPR) of the pristine sample is broader ($\Delta\Omega_{SPR} \approx 1.38$ eV) than for the laser ablated sample ($\Delta\Omega_{SPR} \approx 0.31$ eV) can be attributed to the inhomogeneity of

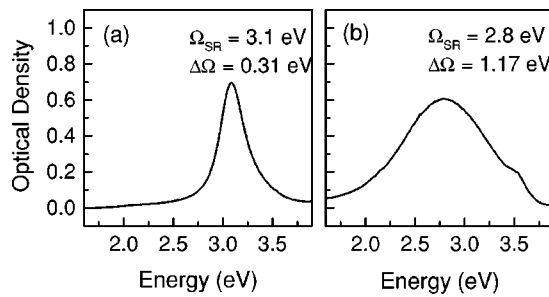


FIG. 1. Linear absorption spectra close to the surface-plasmon resonance for (a) the laser ablated colloid and (b) for the pristine colloid.

either (i) shape or (ii) size distribution of NP. In case (i) a distribution of particles of nonspherical shapes results in a distribution of *SPR* frequencies, due to differences in the depolarization factors.¹⁶ In case (ii) it is known that the Rayleigh approximation is no longer valid for particles with sizes of about 60 nm, and the Mie theory predicts larger widths.^{17,18}

Figure 2(a) shows results of the pump-probe measurements for probe polarization parallel and perpendicular to the pump polarization, for the laser ablated colloid, varying the probe photon energy. The peak around pump-probe delay $\tau = 0$ has a contribution due to four wave mixing, usually called the coherent artifact, which is not of interest here. We focus on the electronic cooling process, which is detected for pump-probe delays greater than ≈ 300 fs, after internal electron thermalization has taken place. We assume the response function for the transient transmission is given by

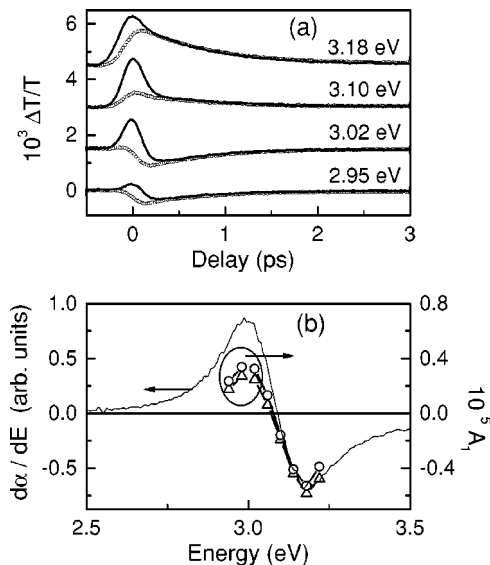


FIG. 2. (a) Transient transmission for the laser ablated colloid, varying the probe photon energy between 2.95 and 3.18 eV, with probe polarization parallel (solid lines) and perpendicular (open circles) to the pump. (b) Amplitudes A_1 obtained by fitting Eq. (1) to the transient transmission, vs probe photon energy, for probe polarization parallel (triangles) and perpendicular (circles) to the pump. The solid line is the derivative of the linear absorption spectra.

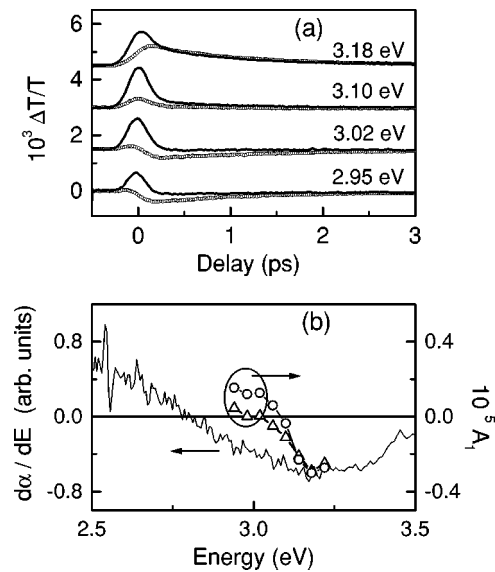


FIG. 3. (a) Transient transmission for the pristine colloid, varying the probe photon energy between 2.95 and 3.18 eV, with probe polarization parallel (solid lines) and perpendicular (open circles) to the pump. (b) Amplitudes A_1 obtained by fitting Eq. (1) to the transient transmission, vs probe photon energy for probe polarization parallel (triangles) and perpendicular (circles) to the pump. The solid line is the derivative of the linear absorption spectra.

$$R_{trans}(t) = \Theta(t)(A_1 \exp^{-t/\tau_{e-ph}} + A_2), \quad (1)$$

where $\Theta(t)$ is the Heaviside function, A_1 and A_2 are the frequency dependent amplitudes, and τ_{e-ph} is the electron cooling time, related to the electron-phonon coupling. Fitting to the experimental signal is performed by convolution of the response function with the normalized cross correlation of the pump and probe pulses. Following this procedure we obtain $\tau_{e-ph} = 730 \pm 30$ fs. In Fig. 2(b) is presented the amplitude A_1 as a function of the probe photon energy for both polarizations. The result is roughly the same in both cases, and can be crudely approximated as the derivative of the linear absorption spectra, which is also shown in Fig. 2(b).

On the other hand, the response for the pristine colloid presents a different behavior both in its relaxation time and the spectral characteristics of the amplitude A_1 , as shown in Fig. 3(a). The relaxation time is approximately the same for both polarizations and equal to $\tau_{e-ph} = 900 \pm 40$ fs. This result is in agreement with the fact that the average size of the NP in the pristine colloid is larger than for the laser ablated colloid. In Ref. 14, it has been demonstrated that the electron-phonon scattering times increase with particle size, and from those results we estimate that the average diameters of the NP in the pristine and laser ablated colloids are >30 nm and ≈ 8 nm, respectively. These estimates are closely correlated to the average particle sizes in our samples, as visualized by electron transmission microscopy.

Figure 3(b) presents A_1 for both perpendicular and parallel polarizations for the pristine colloid. The crossing points for zero amplitude in this sample differ by about 80 meV, with the response for the parallel polarization presenting the lower energy crossing point. As will be discussed later, this is

in qualitative agreement with the fact that for an ellipsoidal NP the SPR frequency polarized parallel to the major axis, Ω_{\parallel} , is smaller than Ω_{\perp} , the resonance frequency for the plasmon polarized perpendicular to the major axis.^{16,18}

We consider that the main aspects of the problem may be described by modeling the NP as ellipsoids of semiaxes $a > b = c$, each with its major axis oriented along an arbitrary direction \hat{n} , and that the dimensions are small compared to the optical wavelengths (Rayleigh approximation). The dielectric constant of the host is supposed real and equal to ϵ_h . In this case, the diagonal polarizability tensor of a single particle in the particle reference frame is given by

$$\alpha'_{jj} = \frac{V[\epsilon(\omega) - \epsilon_h]}{\epsilon_h + L_j[\epsilon(\omega) - \epsilon_h]}, \quad (2)$$

where $\epsilon(\omega) = \epsilon_1 + i\epsilon_2$ is the dielectric constant of the metal, V is the particle volume, and L_j is the depolarization factor.¹⁶ In the case of spherical particles, for example, $L_j = 1/3$ for $j = 1, 2, 3$. If ϵ_2 is small or depends weakly on ω , the plasmon resonances can be obtained from the condition $\epsilon_h + L_j[\epsilon(\Omega_j) - \epsilon_h] = 0$, and the different polarizations of the incident field (relative to the particle reference frame) will sense different resonance frequencies Ω_j . For spherical particles these frequencies are degenerate and polarization independent.

In the photoexcitation process the pump pulse has photon energies that are tuned around $\hbar\omega \approx 1.5$ eV, far from both the interband transition of silver, $\hbar\Omega_{IB} \approx 4$ eV, and the plasmon resonance, $\hbar\Omega_{SPR} \approx 3$ eV. Intraband transitions are responsible for pump pulse energy absorption. The signature of pump-probe experiments for probe energies close to the SPR resembles the derivative of the linear absorption spectra with respect to frequency ω , because of the shift, $\Delta\Omega_j$, and broadening, $\Delta\Gamma_j$, of the plasmon produced by the pump pulse,^{10,12} as observed in Figs. 2(b) and 3(b). The analysis of the temporal behavior of optically excited silver NP follows the general lines discussed in Ref. 11 for spherical particles.

The pump pulse at frequency ω induces a polarization in the particle that in the laboratory reference frame is given by $P_i(\omega) = \alpha_{ij}(\omega)E_j(\omega)$. The probe pulse measures the variation of the transmission at 2ω , which is due to the variation of the polarizability produced by the pump pulse. The variation of the absorbed power of the probe pulse is therefore given by

$$\begin{aligned} \frac{1}{V}\Delta P_{abs}(2\omega) &= -\frac{\omega\epsilon_0}{2} \text{Im}[\Delta\alpha_{ij}(2\omega)E_i(2\omega)E_j(2\omega)], \\ &= -\frac{\omega\epsilon_0}{2} \text{Im}[\Delta\alpha'_{ii}(2\omega)E'_i(2\omega)E'_i(2\omega)]. \end{aligned} \quad (3)$$

The variation of the polarizability is given by

$$\Delta\alpha_{ij} = \frac{\partial\alpha_{ij}}{\partial\epsilon_1}\Delta\epsilon_1 + \frac{\partial\alpha_{ij}}{\partial\epsilon_2}\Delta\epsilon_2. \quad (4)$$

The changes of the real and imaginary parts of the dielectric constants at the probe frequency, $\Delta\epsilon_1$ and $\Delta\epsilon_2$, are assumed to be proportional to the absorbed energy, $\Delta\epsilon_{1,2} \propto \Delta U_{abs} \propto \text{Im}[\vec{P}^*(\omega) \cdot \vec{E}(\omega)]$. Therefore, it is possible to describe the induced absorption changes in terms of a third-order polarization $P_i^{(3)} \propto \chi_{ijkl}^{(3)}(2\omega:2\omega, \omega, -\omega)E_j(2\omega)E_k(\omega)E_l^*(-\omega)$, with

the third-order susceptibility given by $\chi_{ijkl}^{(3)}(2\omega:2\omega, \omega, -\omega) \propto \Delta\alpha_{ij}(2\omega)\alpha_{kl}(\omega)$. Averaging over particle orientation, \hat{n} , must be performed to compare with experimental results. We notice that particle reorientational effects are negligible for the time scales of our measurements. Both $\Delta\alpha_{ij}(2\omega)$ and $\alpha_{kl}(\omega)$ may be calculated once the parameters a , b , and c of the ellipsoid are known. These results are related to the results obtained by Haus *et al.*¹⁹

The physics behind the model for the (anisotropic) pristine colloid may be thus summarized: the pump pulse modifies the dielectric constants of the NP and the induced changes sensed by the probe are due to the particles that have a larger absorption at the pump frequency, ω . This occurs for the ellipsoids oriented parallel to the pump pulse polarization; the particle polarizability is greater for these particles (an extreme limit is the case of a one-dimensional rodlike particle, which only absorbs light polarized parallel to its axis). From electron micrographs of the pristine sample we observe that there is a significant fraction of the NP with aspect ratios as high as $r = a/b = 3$, which would present a ratio of absorption cross sections of the order of $\sigma_{\parallel}/\sigma_{\perp} \approx 40$, at the frequency ω . The probe pulse at 2ω therefore senses predominately the particles that present a hot-electron distribution, which in turn modifies the plasmon resonance in both the directions parallel and perpendicular to the particles' major axis. Each presents the characteristic derivative-like curve in the spectral response, *with different crossing points at the zero derivative line*. For probe polarization parallel to the pump field it is the parallel SPR, Ω_{\parallel} , for a NP with a hot-electron distribution which is probed, while for the perpendicular polarization it is the perpendicular resonance, Ω_{\perp} that is probed, for the same hot-electron distribution.

Another issue to be dealt with is that the size distribution of NP may influence the comparison of the linear and nonlinear spectra presented in Fig. 3(b). To simplify the discussion, we assume that the colloid is composed of only big particles (radius R_b and density n_b) and small particles (radius R_s and density n_s), all of them spherical. We assume the small particles only present the dipole contribution to the absorption coefficient, while big particles present higher-order terms. In this case the linear absorption coefficient will be $\tilde{\alpha}_s \propto n_s R_s^3$, and $\tilde{\alpha}_b \propto n_b R_b^{\gamma}$, with $\gamma < 3$.²⁰

On the other hand, the saturated absorption spectrum presents a different dependence on the particle radius. It can be shown that the variation of the absorption coefficient due to the pump pulse is given by $\Delta\tilde{\alpha}_s \propto n_s R_s^3$, and $\Delta\tilde{\alpha}_b \propto n_b R_b^{2\gamma-3}$. Due to these different dependences with particle radius, it is possible to have a situation in which the linear absorption spectra is dominated by the larger particles in the distribution, while the smaller particles determine the spectral response of the nonlinear absorption spectra. This is what is possibly happening with the pristine colloid: the derivative of the linear absorption spectra in Fig. 3(b) is related to broad SPR resonances, due to big particles,¹⁸ while the nonlinear spectra are dominated by the smaller particles, and is consequently sharper. Of course, the situation is more complex due to the fact that the particles are not spherical, which is also a source of inhomogeneous broadening.¹⁶

In conclusion, polarization-resolved transient absorption measurements in silver colloids have been performed. In a colloid which presents a distribution of nonspherical NP we have shown that it is possible to induce differences in the behavior of the spectra according to the direction in which the probe is polarized relative to the pump beam. These dif-

ferences are accounted for in a model which considers that ellipsoidal particles with their major axis oriented parallel to the pump beam are more polarizable and therefore present a hotter-electron distribution. The parallel and perpendicular components of the pump beam sense different resonances, $\Omega_{\parallel} < \Omega_{\perp}$, as seen in Fig. 3(b).

*Electronic address: lacioli@df.ufpe.br

¹J. Gersten and A. Nitzan, *J. Chem. Phys.* **73**, 3023 (1980).

²G. T. Boyd, Th. Rasing, J. R. R. Leite, and Y. R. Shen, *Phys. Rev. B* **30**, 519 (1984).

³C. K. Sun, F. Vallée, L. H. Acioli, E. P. Ippen, and J. G. Fujimoto, *Phys. Rev. B* **48**, 12365 (1993); **50**, 15337 (1994).

⁴N. Del Fatti, R. Bouffanais, F. Vallée, and C. Flytzanis, *Phys. Rev. Lett.* **81**, 922 (1998).

⁵N. Del Fatti, C. Voisin, M. Achermann, S. Tzortzakakis, D. Christofilos, and F. Vallée, *Phys. Rev. B* **61**, 16956 (2000).

⁶J. -Y. Bigot, J. -C. Merle, O. Cregut, and A. Daunois, *Phys. Rev. Lett.* **75**, 4702 (1995).

⁷T. V. Shahbazyan, I. E. Perakis, and J. -Y. Bigot, *Phys. Rev. Lett.* **81**, 3120 (1998).

⁸J. -Y. Bigot, V. Halté, J. -C. Merle, and A. Daunois, *Chem. Phys.* **251**, 181 (2000).

⁹J. H. Hodak, I. Martini, and G. V. Hartland, *J. Phys. Chem.* **102**, 6958 (1998).

¹⁰Y. Hamanaka, N. Hayashi, A. Nakamura, and S. Omi, *J. Lumin.* **76&77**, 221 (1998).

¹¹N. Del Fatti, F. Vallée, C. Flytzanis, Y. Hamanaka, and A. Nakamura, *Chem. Phys.* **251**, 215 (2000).

¹²C. Voisin, N. Del Fatti, D. Christofilos, and F. Vallée, *J. Phys. Chem.* **105**, 2264 (2001).

¹³C. Voisin, D. Christofilos, N. Del Fatti, F. Vallée, B. Prével, E. Cottancin, J. Lermé, M. Pellarin, and M. Broyer, *Phys. Rev. Lett.* **85**, 2200 (2000).

¹⁴A. Arbouet, C. Voisin, D. Christofilos, P. Langot, N. Del Fatti, F. Vallée, J. Lermé, G. Celep, E. Cottancin, M. Gaudry, M. Pellarin, M. Broyer, M. Maillard, M. P. Pileni, and M. Treguer, *Phys. Rev. Lett.* **90**, 177401 (2003).

¹⁵P. C. Lee and D. Meisel, *J. Phys. Chem.* **86**, 3391 (1982).

¹⁶H. Kuwata, H. Tamaru, K. Esumi, and K. Miyano, *Appl. Phys. Lett.* **83**, 4625 (2003).

¹⁷K. L. Kelly, E. Coronado, L. L. Zhao, and G. C. Schatz, *J. Phys. Chem.* **107**, 668 (2003).

¹⁸M. Scharte, R. Porath, T. Ohms, M. Aeschlimann, J. R. Krenn, H. Ditlbacher, F. R. Aussenegg, and A. Liebsch, *Appl. Phys. B: Lasers Opt.* **B73**, 305 (2001).

¹⁹J. W. Haus, R. Inguva, and C. M. Bowden, *Phys. Rev. A* **40**, 5729 (1989).

²⁰H. C. van de Hulst, *Light Scattering by Small Particles* (Dover, New York, 1981).